energies

MDPI

Article

Optimum Organic Rankine Cycle Design for the Application in a CHP Unit Feeding a District Heating Network

Lisa Branchini, Andrea De Pascale *, Francesco Melino and Noemi Torricelli

Department of Industrial Engineering, Alma Mater Studiorum—Università di Bologna, viale del Risorgimento 2, 40136 Bologna, Italy; lisa.branchini2@unibo.it (L.B.); francesco.melino@unibo.it (F.M.); noemi.torricelli2@unibo.it (N.T.)

* Correspondence: andrea.depascale@unibo.it; Tel.: +39-051-2093310

Received: 28 February 2020; Accepted: 10 March 2020; Published: 12 March 2020

Abstract: Improvement of energy conversion efficiency in prime movers has become of fundamental importance in order to respect EU 2020 targets. In this context, hybrid power plants comprising combined heat and power (CHP) prime movers integrated with the organic Rankine cycle (ORC) create interesting opportunities to additionally increase the first law efficiency and flexibility of the system. The possibility of adding supplementary electric energy production to a CHP system, by converting the prime movers' exhaust heat with an ORC, was investigated. The inclusion of the ORC allowed operating the prime movers at full-load (thus at their maximum efficiency), regardless of the heat demand, without dissipating not required high enthalpy-heat. Indeed, discharged heat was recovered by the ORC to produce additional electric power at high efficiency. The CHP plant in its original arrangement (comprising three internal combustion engines of 8.5 MW size each) was compared to a new one, involving an ORC, assuming three different layout configurations and thus different ORC off-design working conditions at user thermal part-load operation. Results showed that the performance of the ORC, on the year basis, strongly depended on its part-load behavior and on its regulation limits. Indeed, the layout that allowed to produce the maximum amount of ORC electric energy per year (about 10 GWh/year) was the one that could operate for the greatest number of hours during the year, which was different from the one that exhibited the highest ORC design power. However, energetic analysis demonstrated that all the proposed solutions granted to reduce the global primary energy consumption of about 18%, and they all proved to be a good investment since they allowed to return on the investment in barely 5 years, by selling the electric energy at a minimum price equal to 70 EUR/MWh.

Keywords: organic Rankine cycle; waste heat recovery; internal combustion engine; cogeneration; district heating

1. Introduction

In the framework of the "20–20–20" targets [1], measures adopted by the European Union to mitigate climate change include the improvement of conventional prime movers' conversion efficiency. As indicated in the European directive 2012/27/EU [2], the promotion of cogeneration, as well as waste heat recovery (WHR) strategies, could significantly contribute to achieving this objective.

Internal combustion engines typically convert just the 30–45% of the fuel primary energy into mechanical or electric power, while the remaining part is rejected as thermal energy with exhaust gases, cooling water, oil, etc. This heat, which would be wasted otherwise, can be used for combined heat and power (CHP) applications, thus improving the overall first law conversion efficiency, but also

for additional electric production, via a bottomer thermodynamic cycle. Heat released by internal combustion engine (ICE) exhaust gases is usually characterized by (i) limited thermal power size (varying typically in the range from kW to tens of MW as order of magnitude), (ii) by temperature often quite lower than 500 °C, and (iii) both strongly variable with the engine load. These conditions are not always compatible with the adoption of conventional steam Rankine cycle [3] since problems related to the use of water as working fluid can arise as (i) difficulty in superheating the fluid in order to avoid condensate formation during the expansion process and the risk of erosion of the turbine blades [3]; (ii) working with excessive vapor operating pressure that impose to install complex multi-stage and expensive turbines [3]. A solution is identified in changing the operating fluid with an organic compound in an organic Rankine cycle (ORC). Organic fluids are characterized by higher molecular mass and lower critical temperature compared to water that allows exploiting efficiently, also, low-grade heat sources. Even though the conversion efficiency of ORC is typically limited, compared to steam cycle, this technology features a number of advantages: lower O&M and personnel costs; high molecular weight; low enthalpy drop in the expander, and, as a consequence, higher mass flow rates, if compared with water. Moreover, ORCs are characterized by a wider regulation range, and performances are not particularly penalized at part-load conditions [4].

WHR from stationary ICE prime movers is quite a consolidated option, and several investigations have been proposed on this topic (see for example [5–14]). The studies point out that ORC performance is significantly affected by the choice of the working fluid, the cycle architecture, and the setting of the operating parameters. Investigated fluids are hydrocarbons, refrigerants, and zeotropic mixtures, while the other most important decision variables are identified in the evaporating pressure and the superheating degree [5–7]. In particular, Yang et al. analyzed an ORC system in [5] to recover waste heat from the diesel engine exhaust, where the zeotropic mixture R416A was used as the working fluid for the ORC. Considering various operating conditions of the diesel engine, this study investigated the effects of the degree of superheating on the running performance of the ORC waste heat recovery. In the thermodynamic study by Han et al. [6], a regenerative ORC system was established to recover the waste flue gas of 160 °C, focusing on thermodynamic and economic performance while simultaneously considering the effect of superheating and working fluid selection. The optimization of the evaporation temperature was carried out by analyzing the variation of net power output and specific investment cost. Energy and exergy analysis of three ORC–WHR configurations that use a coupling thermal oil circuit was performed by Valencia et al. in [7], where a simple ORC, an ORC with a recuperator, and an ORC with double-pressure configuration were considered; cyclohexane, toluene, and acetone were simulated as ORC working fluids. In addition, the effect of evaporating pressure on the net power output, thermal efficiency increase, specific fuel consumption, overall energy conversion efficiency, and exergy destruction was also investigated.

These studies demonstrated also the importance of taking into account the part-load operation of the ICEs when evaluating the performance of the ORC bottoming solution. For example, in [8] and [9], the performance of combined systems with ORC and ICE was analyzed at steady-state under different typical working conditions, by means of a numerical simulation model of the system. These papers analyzed, in addition, the effect of adjustable parameters on the system performance, giving effective control directions under various conditions. They proved that to get a better system performance under different working conditions, the system should be operated with a slight degree of superheating.

Valorization of waste heat through ORC creates interesting opportunities, especially to combined heat and power generation, in the residential sector and in energy-intensive industries. In this context, a series of hybrid power plants comprising a CHP prime mover integrated with ORC have been investigated [10–13], with the aim of maximizing the share of electricity production of CHP plants rather than a higher heat production rate in a cost-effective manner. The analyzed heat sources are usually cooling water from steam cycles or exhaust gas from the industrial process. An example of a hybrid CHP plant was proposed by Yi et al. in [10], where an ORC and a hydraulic turbine were introduced to reduce exergy losses, which occurred in a thermal storage process for district heating (DH) purpose.

Results showed a payback period equal to just 3.5 years. The study proposed by Arabkoohsara and Namib [11] analyzed a waste-driven CHP plant. In addition to the electricity generated by the main steam cycle, the heat withdrawn from the condenser was employed for additional heat and electricity production by employing a small-scale ORC unit and a heat exchanger connected to the local district heating system. This study evaluated an electric efficiency improvement of 20% and a favorable period of return on investment. Marty et al. [12] analyzed the optimization of parallel distribution between electricity and heat production for a geothermal plant. The geothermal fluid was split into two streams, one used for an ORC system, and the other for the DH. An optimization tool was implemented to obtain the sizing of the ORC and the best distribution between electricity and heat production. In the project by Ramireza et al. [13], a large-scale ORC pilot plant along with a waste heat recovery unit in a steel mill was designed. Waste heat was recovered from the fumes of the furnace to produce saturated steam, which was then delivered to a DH network during the cold season and to the ORC for electricity generation during the rest of the year. Results on the performance of the plant during the first months of operation showed promising values. The study by Grljušić et al. [14] showed instead an application involving a diesel engine for maritime application. A standard operating propulsion engine at maximum efficiency was assumed to supply the auxiliary power. The aim of this research was to investigate the possibility of using the CHP plant over a ship to meet all heating and electricity requirements during navigation.

All these studies make evident that the ORC design for CHP hybrid systems has to be determined in accordance with the specific application. In particular, in the case of a CHP ICE-ORC hybrid system, the optimal ORC sizing, the optimal load allocation, and the resulting off-design performance should be explored more in depth, especially if it is called to operate under variable thermal demand conditions.

The Objective of the Study

The main objective of this work was the energy and economic assessment of a CHP power plant based on ICEs, feeding a DH network, and coupled with an ORC to optimally recover the ICEs' residual heat. In this work, a specific case study of an existing CHP system was analyzed; however, the same presented approach and similar considerations could be applied to any CHP feeding a district heating network (DHN) as a thermal user.

In detail, as the first step, the optimal operation of the CHP power plant was assessed without ORC: the ICEs load profile was determined, in order to fulfill the DH thermal demand, while minimizing the heat dissipation to the ambient. Then, in order to increase the amount of produced electrical energy and to better exploit the available ICEs residual heat, the opportunity of integrating an ORC as a bottomer was investigated.

The original power plant optimal operation was compared with the new arrangement, where the ICEs were operated at full-load, and the ORC was integrated also with the DH demand, to recover the ICEs' residual heat. The ORC as bottomer of the CHP was an interesting solution also because it could represent a flexibilization tool in the regulation of the whole plant. The ORC allowed operating the ICEs at full-load (i.e., at maximum efficiency point) while not dissipating the surplus of heat production when it is not required by the thermal user. Indeed, the surplus of high enthalpy-heat production was recovered by the ORC and converted into additional electric power, sold to the electric grid.

In detail, three different system architectures were proposed and analyzed. A sensitivity analysis of organic fluid and key cycle parameters was performed in order to identify, for each proposed arrangement, the optimum design of the ORC. A thermodynamic design and off-design model of the ORC system has been developed in the *Thermoflex*™ environment [15]. The additional electrical energy produced during the year, the ORC operating hours, and total investment costs were quantified and compared among the analyzed layouts. Finally, the original optimal operation of the CHP plant was compared with the modified one comprising the ORC, in order to estimate, for each proposed arrangement, the amount of additional generated electric power and the corresponding increase in primary energy consumption.

An energetic index accounting for the global primary energy saving was introduced, in order to evaluate the convenience in producing the additional electric power with the modified CHP plant rather than with the original plant with the help of the electric generating mix. From the economic point of view, considerations on the electric energy sell price to return on investment were also presented.

2. Cogeneration Power Plant Description

This section presents the description of the CHP plant feeding the DH network and the control logic adapted to regulate the system when working at part-load conditions.

2.1. CHP Plant Arrangement

The case study system was an existing cogeneration plant intended to satisfy the heat demand of an international hub airport; it comprised three ICEs (model Rolls Royce Bergen engine B35: 40 V20 AG), fed with natural gas, named GR1, GR2, and GR3, as depicted in Figure 1. The CHP single unit prime movers were conceived to provide a nominal electric power equal to 8.5 MW and thermal power of about 4.6 MW (only heat recovery from the exhaust gas is considered). Thus, the nominal electric and thermal efficiency were equal to 47% and 25%, respectively. The DH demand was fulfilled by the ICEs discharged heat and by three additional boilers, producing 8 MW of nominal thermal power output each, also fed with natural gas. The generated electric power was fed into the grid at a connection voltage of 150 kV.

The DH network (DHN) was designed to provide hot water for various types of tertiary building users. It included heat exchangers for heating purposes in winter and heat exchangers working all along the year, providing high-temperature heat to produce food use steam and to feed absorption refrigeration units, but also sanitary water.

For what regards the management strategy, a DHN could be regulated (i) varying the mass flow rate but keeping constant the temperature difference (ΔT) on the utilities (this approach is particularly suitable for small size DHNs) or (ii) varying the ΔT on the utilities with a constant mass flow rate (usually for large DHNs) [16]. The regulation adopted in this study was the first one: in particular, it was assumed that the delivery temperature was kept equal to 130 °C and the return equal to 70 °C. This supposition could be reasonable if considering that the DHN inertia was typically such high to presume to be neglectable the return temperature oscillation when relying on an hourly basis (which was the timestep considered in this analysis).

The yearly required thermal production profile is shown in Figure 2. Higher thermal power requests were observed during winter, with a demand peak close to 20 MW; lower heat demand values, around 3 MW on average, were registered during summer months.

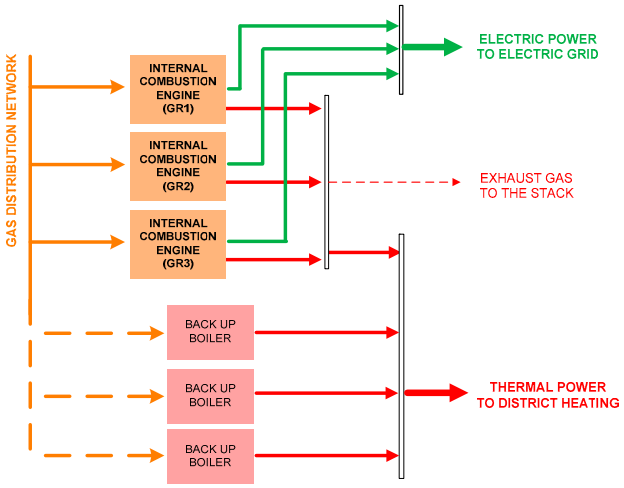

Figure 1. Schematic of the cogeneration power plant.

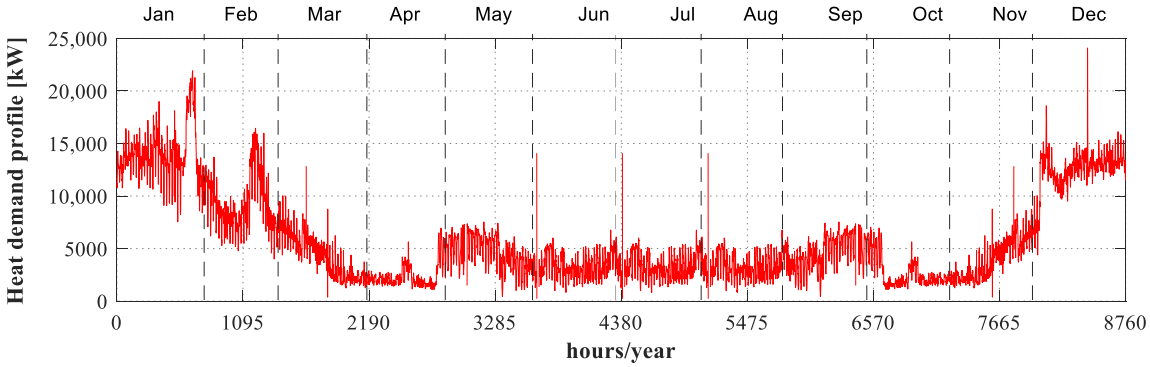

Figure 2. Heat demand yearly profile.

2.2. CHP Plant Control Logic

The control logic of the CHP plant was defined based on the result of an optimal load allocation procedure, which led to defining the optimal ICE single unit load for each value of the heat demand. The optimal load allocation problem was formulated as follows (Equation (1)): CHP prime movers were managed in order to cover the DH demand ($\dot{Q}_{th,DH}$) while keeping equal to zero the heat dissipation to stack ($\dot{Q}_{th,Diss}$), with the following constraints: (i) the ICE regulation ranges in between 40% to 100% of the nominal load (according to ICE datasheet); (ii) minimum exhaust gas temperature ($T_{exhaust}$) equal to 110 °C [17], as conservative value, to prevent water condensation along the discharge line; (iii) when a potential ICE heat dissipation would occur, the boilers are turned on to cover the heat demand, in place of the ICEs, in order to avoid high-grade enthalpy wasted heat.

$$\dot{Q}_{th,Diss}(\overline{x}) = 0 \; such \; that \begin{cases} \dot{Q}_{th,PM}(\overline{x}) = \dot{Q}_{th,DH} \; if \; \dot{Q}_{th,DH} < \dot{Q}_{th,PM,max} \\ \dot{Q}_{th,PM}(\overline{x}) = \dot{Q}_{th,PM,max} \; if \; \dot{Q}_{th,DH} \geq \dot{Q}_{th,PM,max} \\ T_{exhaust}(\overline{x}) = 110 \; ^{\circ}\mathrm{C} \\ 0.4 \; \leq \overline{x} \leq 1 \end{cases} \quad (1)$$

$$\overline{x} = load_{GR1}, load_{GR2}, load_{GR3}$$

where the problem control variables ($\overline{x}$) are the three ICE loads ($load_{GR1}$, $load_{GR2}$, $load_{GR3}$). The resulting optimization problem could be treated as a constrained, multivariable function, minimization problem.

The problem was solved considering the heat demand profile (Figure 2) and the ICE and boiler performance maps (Figure 3). The boiler efficiency trend describes the part-load behavior of a boiler conceived for the auxiliary purpose [18], thus characterized by high performance, even at very low loads. In particular, Figure 3 shows the ICE exhaust gas mass flow rate and temperature, the electrical and thermal power output versus load (data provided by the manufacturer). The thermal power was calculated, assuming cool exhaust gases down to 110 °C. It resulted that each ICE could be regulated between the 40 and the 100% of its load, covering a heat demand ranging between 3200 and 4600 kW; thus, the three ICEs together could cover a maximum heat demand equal to 13,800 kW.

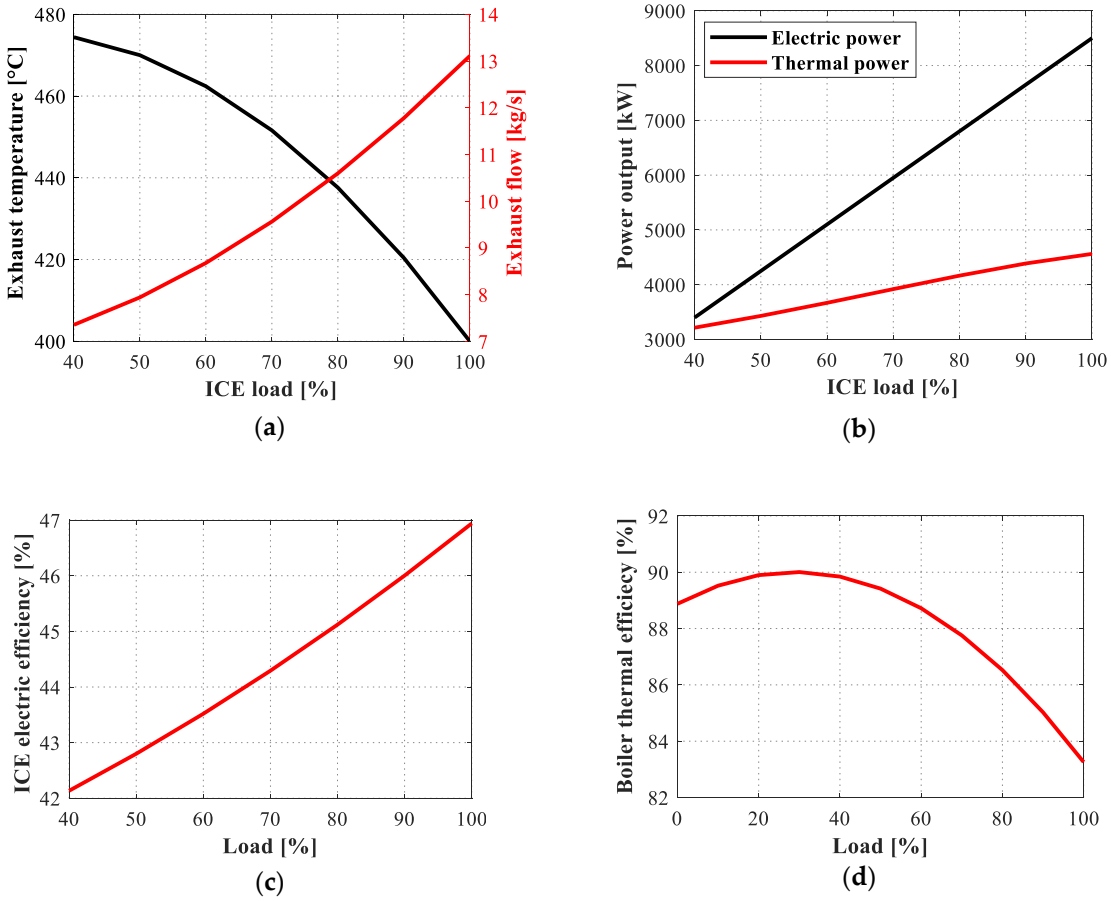

Figure 3. Performance of internal combustion engines (ICEs) and back-up boilers at part-load conditions: (**a**) ICE exhaust gas conditions at part-load operation; (**b**) ICE electric and thermal power output at part-load operation; (**c**) ICE electric efficiency at part-load operation; (**d**) Boilers thermal efficiency at part-load operation.

Results of optimal load allocation procedure are reported in Figure 4, where the load of the three ICE units (Figure 4a), the CHP unit total electric power output (Figure 4b), and boilers load (Figure 4c) as a function of the heat demand are shown. Finally, in Figure 4d, the total natural gas consumption (due to ICE units and boilers) was plotted versus the heat demand. It could be observed that, in the range of power where the ICEs operated, only the least number of units necessary to cover the demand was activated. They were turned on at their minimum load, and then the load increased with the heat demand until reaching 100%. Beyond 13,800 kW, all the ICEs worked at full-load, but the generated power was not enough to cover the heat demand; therefore, also the back-up boilers were activated. The boilers were activated also at heat demand lower than 13,800 kW when the ICEs could not fulfill the heat demand due to the regulation limits expressed in (1).

The total amount of natural gas consumed to fulfill the DH yearly heat demand resulted equal to 138.36 GWh/year; it guaranteed to cover the heat demand and to deliver 54.22 GWh/year of electric power to the grid. The ICE and the boiler fuel consumption were evaluated on the basis of the efficiency maps reported in Figure 3c,d.

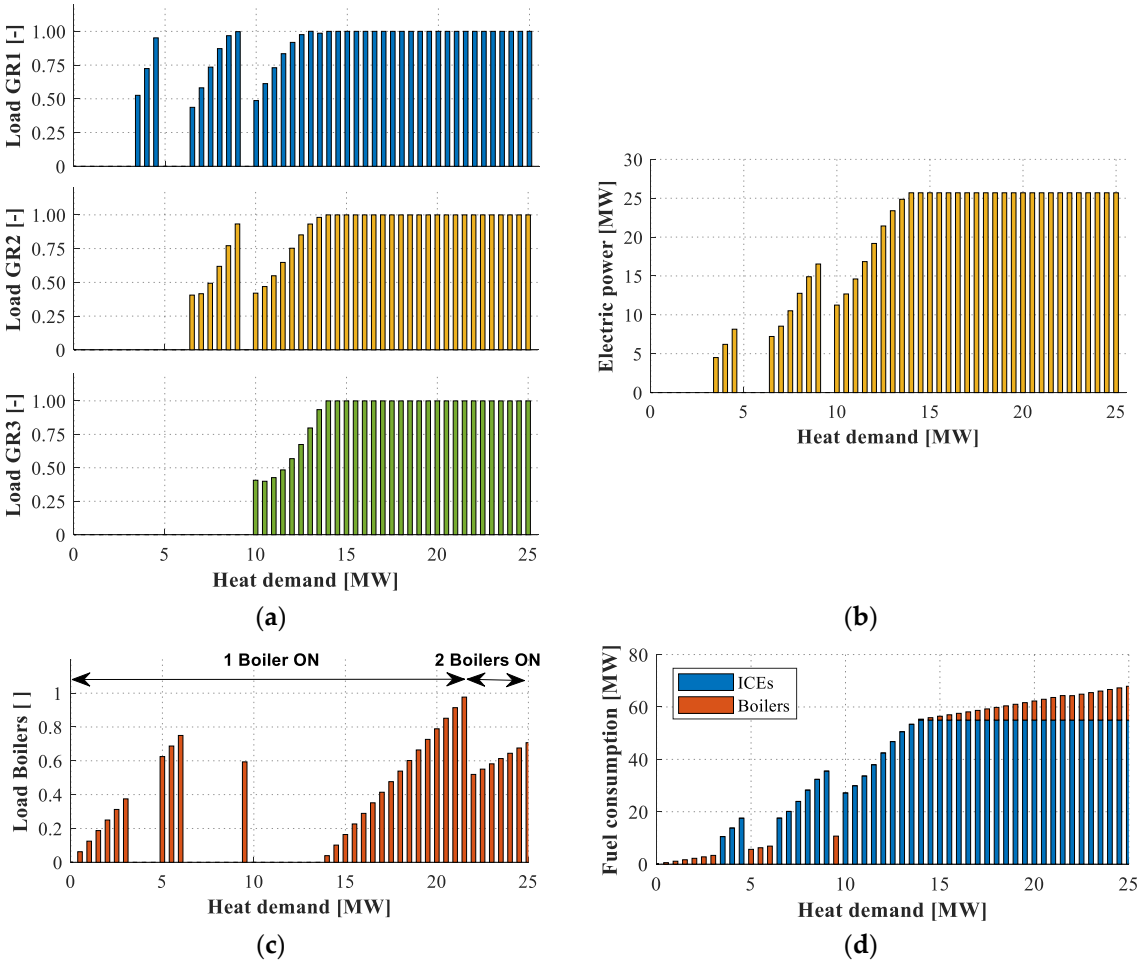

Figure 4. Combined heat and power (CHP) system output loads and fuel consumption as a function of the district heating (DH) heat demand: (**a**) load of the ICE units; (**b**) CHP unit total electric power output; (**c**) boilers load as a function of the heat demand; (**d**) total natural gas consumption.

3. Integrating the Organic Rankine Cycle

In order to increase the amount of electrical energy sold to the grid, the opportunity of integrating an ORC as a bottoming cycle of the ICEs was considered. Since ORC technology offers the possibility to generate electricity from low-grade heat sources, the residual heat of ICEs exhausts flue gases was here considered as a potential feeding source. Thus, the CHP plant optimal operation was compared with a new arrangement where ICEs were operated at full-load, and an ORC was integrated into the layout to recover ICEs' residual heat. Three different ICE-ORC layouts were proposed and analyzed. For each investigated arrangement, optimum ORC design (i.e., selection of organic fluid and key cycle parameters) was identified; based on ORC system off-design modeling, the amount of additional electrical energy producible during the year was then quantified.

3.1. ORC Architecture

A simple sub-critical and regenerative ORC architecture with an intermediate heat transfer fluid (IHTF) loop was assumed, as schematically shown in Figure 5. The key cycle components were: (i) the heat exchanger between ICE exhaust gases and heat carrier fluid, (ii) the evaporator (exchanging heat between the heat carrier fluid and organic fluid), (iii) the expander, (iv) the regenerative heat exchanger, and (v) the condenser and pumps. The use of an intermediate thermal circuit, which could act as buffer, was crucial for the application under consideration in order to: (i) avoid the direct contact between

exhaust gases and flammable organic fluid (such as hydrocarbon), (ii) smooth out the variation of temperature and mass flow rate of the heat source.

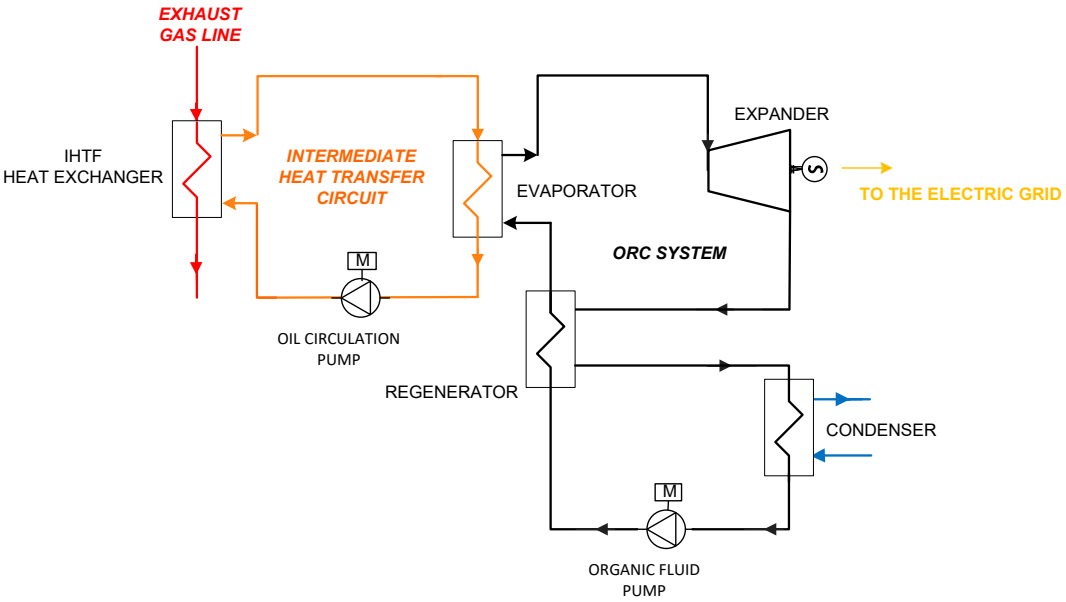

Figure 5. Schematic of the organic Rankine cycle (ORC) architecture.

3.2. *Proposed Series and Parallel Arrangements*

Three different layouts were investigated in this work, as schematically shown in Figure 6.

In the first case (Case A), the ORC was placed downstream the heat exchanger feeding the DH network, thus recovering the residual heat of exhausted gases. Therefore, the DH heat demand would determine the temperature of the gas feeding the ORC.

In the second architecture (Case B), the heat recovery heat exchanger position was reversed, with the ORC located upstream of the DH heat exchanger. Accordingly, in this second arrangement, the ORC would be fed by a constant temperature, equal to 400 °C (i.e., the temperature of ICE exhausted at full-load condition, see Figure 3a), while the total amount of heat input to the cycle would vary, according to the DH request.

In the third analyzed layout (Case C), a parallel arrangement was assumed: exhaust gas flow would be split between the two branches in order to primarily satisfy the DH load demand, while both branches featured the same inlet gas temperature value (equal to 400 °C). A collector was placed downstream components, in order to mix up the two different fluxes; the minimum requirement of 110 °C on temperature was maintained in section G3 of Figure 6.

Indeed, for all the above described integrated system architectures, the heat demand of DH was the primary requirement to meet. Consequently, the thermal power input to the ORC equaled the difference between the available thermal power in the ICE exhaust gas and heat delivered to the DH network ($\dot{Q}_{th,DH}$). For each investigated layout, Table 1 collects the assumed constant and variable parameters (see the section in Figure 6). The intermediate heat transfer fluid heat exchanger, which provided the thermal power input to the ORC, was indicated as IHTF HE for the sake of brevity.

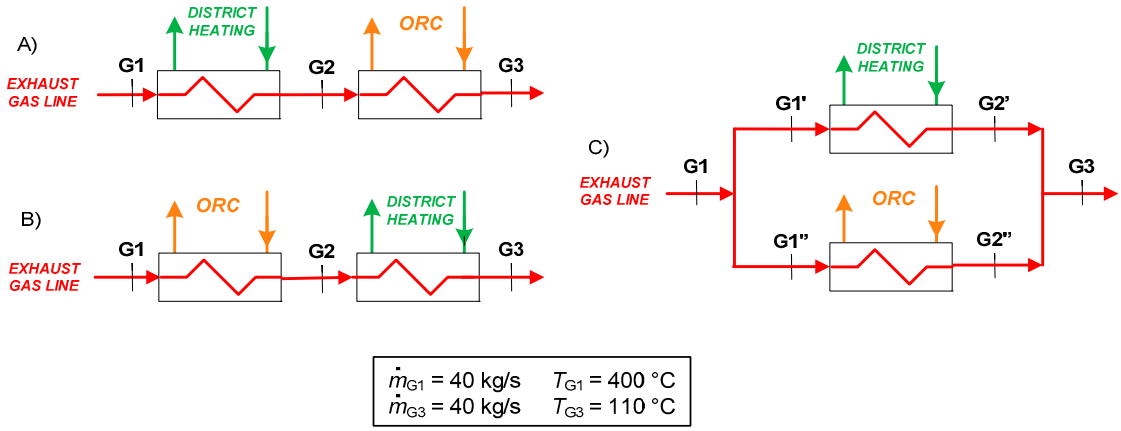

Figure 6. Schematic of the proposed DH and intermediate heat transfer fluid (IHTF) heat exchangers arrangements: (**a**) case A; (**b**) case B; (**c**) case C.

Table 1. Constants and variable parameters for each proposed layout.

Layouts	Case A	Case B	Case C
Exhaust gas mass flow rate entering the IHTF HE	$\dot{m}_{G2} = 40$ kg/s	$\dot{m}_{G1} = 40$ kg/s	$\dot{m}_{G1''} = f(\dot{Q}_{th,DH})$
Exhaust gas temperature entering the IHTF HE	$T_{G2} = f(\dot{Q}_{th,DH})$	$T_{G1} = 400$ °C	$T_{G1''} = 400$ °C
Outlet gas temperature at the IHTF HE	$T_{G3} = 110$ °C	$T_{G2} = f(\dot{Q}_{th,DH})$	$T_{G2''} = 110$ °C

3.3. Selected Organic Working Fluids

Four different hydrocarbons (Cyclopentane, Benzene, Cyclohexane, and Toluene) were selected as potential working fluids, as demonstrated to be performing fluids for recovering heat at the temperature imposed by the ICEs exhausts [19,20]. Indeed, the selected fluids exhibited a critical temperature quite similar or slightly higher than the target evaporation temperature, in particular high enough to achieve a good thermal matching between fluids and exhaust gas, but not too high to lead to excessively low vapor densities and thus high system cost [21]. Refrigerants were excluded due to their low critical temperature, while siloxanes were excluded because their use would lead to excessively low saturation pressure values, assuming cooling fluid temperature close to ambient conditions [21]. The main properties of selected fluids are summarized in Tables 2 and 3, and the fluids saturation pressure values are plotted versus temperature for comparative purpose in Figure 7.

The IHTF considered was Therminol 62, one of the most popular high-temperature liquid phase heat transfer fluid. Therminol 62 was selected as it offers outstanding performance to 325 °C, including excellent thermal stability and low vapor pressure. These properties result in reliable, consistent performance of heat transfer systems over long periods of time (main properties are reported in Table 3) [22].

Table 2. Main properties of selected organic fluids [21].

Organic Fluid Property	Cyclopentane	Benzene	Cyclohexane	Toluene
Molar weight (kg/kmol)	70.1	78.1	84.2	92.1
Critical pressure (bar)	45.8	49.1	40.8	41.3
Critical temperature (°C)	238.6	288.9	280.5	318.6
Normal boiling point (°C)	49.3	80.1	80.7	110.6
Autoignition temperature (°C)	320	555	260	480

Table 3. Main properties of selected IHTF [22].

IHTF Property	Therminol 62
Molar weight (kg/kmol)	252
Normal boiling point (°C)	333
Autoignition temperature (°C)	433
Liquid density at 25 °C (kg/m^3)	951

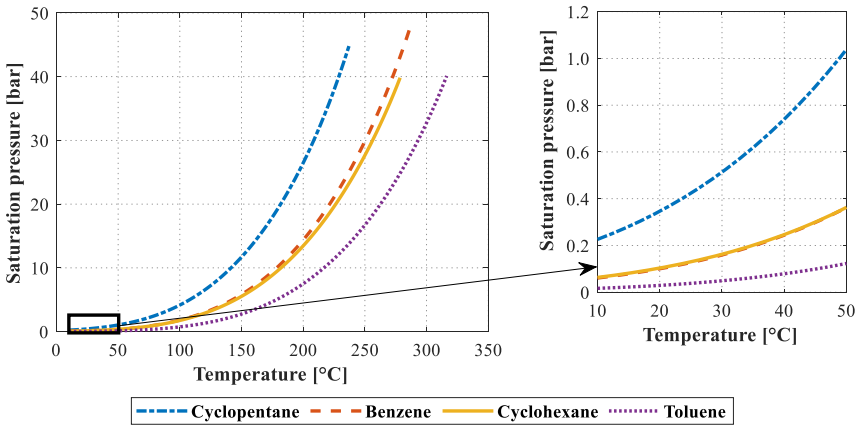

Figure 7. Pressure-temperature saturation curves of selected hydrocarbons.

3.4. ORC Thermodynamic Modeling and Design Assumptions

The ORC system and the IHTF circuit were modeled and simulated by means of the commercial software *Thermoflex*™ [15]. The software, integrated with the FluidProp library for organic fluids thermodynamic properties evaluation, allowed simulating the energy system steady state, based on a lumped parameters approach.

First of all, the whole system layout was reproduced in the *Thermoflex*™ environment, combining the built-in library single component modules of heat exchangers, turbines, pumps, sources, and sinks. Boundary conditions and components design key parameter values used in the study (such as turbine isentropic efficiency, condensation pressure, pressure drops, and heat losses along the circuit) are listed in Tables 4–6, mainly selected in line with the state-of-the-art of conventional ORC technology [23].

Table 4. ORC layouts dependent assumptions.

Layout CASE	A1	A2	A3	B	C
Exhaust gas temperature entering the IHTF HE (°C)	342 (G2)	342 (G2)	342 (G2)	400 (G1)	400 (G1″)
Exhaust gas mass flow rate entering the IHTF HE (kg/s)	40 (G2)	40 (G2)	40 (G2)	40 (G1)	32 (G1″)
Outlet gas temperature exiting the IHTF HE (°C)	110 (G3)	110 (G3)	110 (G3)	208 (G2)	110 (G2″)
IHTF temperature (T_{des}) (°C)	300	250	200	300	300

Table 5. ORC general assumptions.

General Assumption	
Pressure drop at the heat exchangers (%)	10
Heat exchangers thermal loss (%)	1
IHTF loop max. pressure (bar)	15 15
Pressure drop in IHTF loop (%)	15
ORC expander isentropic efficiency (%)	80 80
Regenerator effectiveness (%)	85
Subcooling ORC outlet condenser (°C)	5
Pumps nominal isentropic efficiency (%)	60

Table 6. ORC condensation pressure assumptions.

Fluids	Condensation Pressure (Bar)
Cyclopentane	0.74
Benzene	0.24
Toluene	0.08
Cyclohexane	0.25

In order to perform a realistic evaluation of the ORC performance, both thermodynamic design and off-design analyses were performed. Off-design performance of the plants were obtained passing through three main steps: (i) preliminary thermodynamic heat and mass balances; (ii) engineering design phase, in which design parameters of the power plant are defined (i.e., size of components, geometric details, etc.); (iii) thus, off-design analysis where, being defined the design characteristics and fixed the geometry of the components, depending on selected control logic, it is possible to predict both components and overall system behavior under different operating conditions.

The main equations used to calculate streams' design parameters included energy balances at the single components. A more exhaustive description of the Thermoflex modeling approach can be found in [23]. Concerning the off-design modeling approach, the heat exchangers off-design behavior was calculated according to the method of thermal resistance scaling [15]. Being determined as the design-point overall thermal resistance of the heat exchanger, the two fluid-side resistances were scaled at off-design, using the single-parameter scaling method [15]. Normalized heat loss in each heat exchanger was considered, and it was entered as a percentage, relative to the heat transferred out of the higher temperature fluid. Flow resistance coefficients, initialized in the design-point stage, were used to model the pressure drops across each side of the heat exchanger in off-design. Regarding the ORC expander, the sliding pressure part-load control was assumed to model its behavior at off-design conditions. Thus, whenever possible (based on topper off-design performance), the organic fluid temperature at the expander inlet was kept constant at its rated design value, while mass flow and pressure varied proportionally assuming chocking conditions (constant mass flow function) at the turbine inlet. Expander isentropic efficiency at off-design was corrected, starting from the design point value, based on flow function.

Table 4 shows the selected design values for the inlet/outlet temperature and mass flow of the gas at the IHTF HE, for the different proposed layouts; these values corresponded to a DH demand equal to 3 MW, the mean value of the thermal demand in the period of minimum request (May to September). The IHTF circuit design temperature at the HE outlet (T_{des}) was set equal to 300 °C in Case B and Case C layouts, while three possible values (Case A1: 200 °C, Case A2: 250 °C, and Case A3: 300 °C) were considered in Case A layout, where the IHTF HE was downstream the DH HE.

The condensation pressure depends on the working fluid, and it is bound by the cold source temperature. In this study, the cooling medium temperature was assumed equal to 25 °C as representative of a medium climate condition [24]. Considering a reasonable temperature difference

between organic fluid saturation temperature and cooling medium temperature inlet equal to 15 °C, the organic fluid condensation temperature was set equal to 40 °C for all considered fluids, resulting in the condensation pressure values in Table 6 (see also Figure 7). In order to guarantee a complete fluid condensation inside the condenser, a subcooling equal to 5 °C was assumed.

4. Results and Discussion

4.1. Optimization of the Cycle Parameter and Working Fluid Selection

A preliminary thermodynamic sensitivity analysis was performed on the considered working fluids, in order to optimize the cycle evaporation pressure and then determine the fluid that maximizes the net electric power production, for each analyzed arrangement.

The influence of organic fluid and key cycle operating parameters are presented in Figure 8, with reference to Case A layout. Since the exhaust gas entering the IHTF HE was variable in case A (see Table 1), a comparative analysis of the net power output is presented in Figure 8 for each analyzed T_{des} value and for each organic fluid. Results showed that Cyclopentane achieved the best performance compared to other hydrocarbons, for all the considered T_{des} values. However, it must be pointed out that ORC performance was reduced by decreasing the IHTF temperature. Optimum evaporation pressure values could be identified equal to 40, 16, and 10 bar, respectively, at 300, 250, and 200 °C. As expected, the highest ORC performance was achieved for the highest temperature (i.e., 1490 kW of net power output for Cyclopentane with a pressure equal to 40 bar and T_{des} equal to 300 °C). If the design IHTF temperature was reduced to 200 °C, the maximum ORC power output was reduced by nearly 20%.

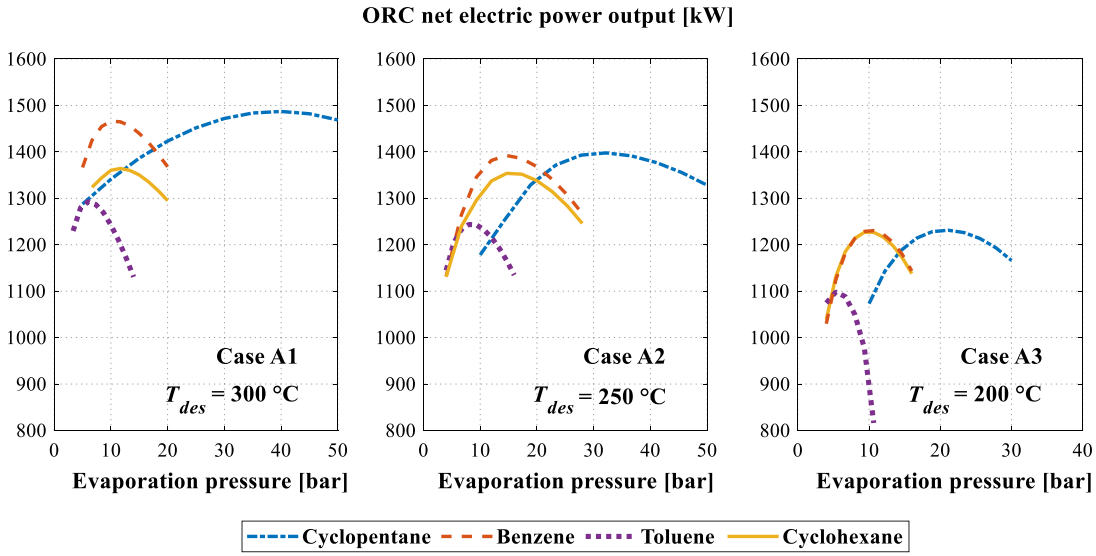

Figure 8. Sensitivity analysis results on organic fluid and IHTF design temperature in Case A layout and different IHFT temperature cases.

Figure 9 shows the results for Case B and Case C: a fixed IHTF design temperature value equal to 300 °C was considered. Indeed, these proposed layouts featured the maximum temperature of exhaust gas entering the IHTF HE (T_{G1} and T_{G1}", respectively, see Table 1). Cyclopentane still provided the best performance in Case B and Case C layouts. The maximum power output was achieved with evaporation pressure equal to 40 bar for both layout arrangements. The highest ORC power output value was obtained in Case B, in which the IHTF HE was fed with the exhaust gas at its highest temperature and mass flow if compared with the other cases.

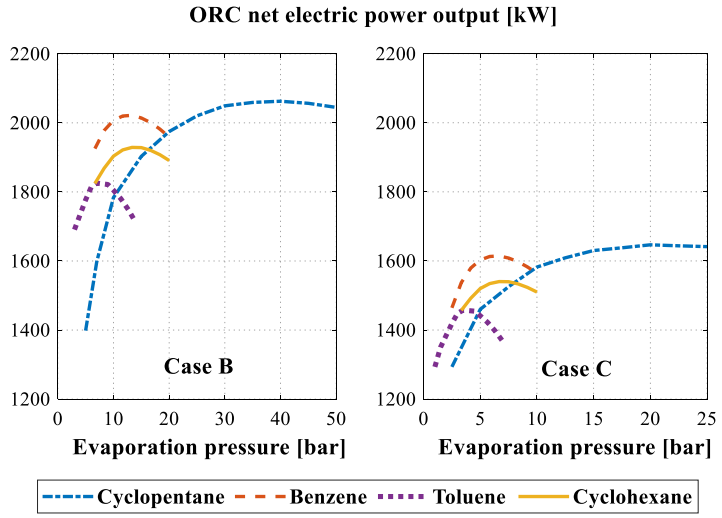

Figure 9. Sensitivity analysis results on organic fluid and IHTF design temperature: Case B and Case C layout.

4.2. Off-Design Analysis

Based on sensitivity analysis results and design assumptions of Tables 4–6, off-design evaluation of proposed layouts was carried out, considering Cyclopentane as working fluid in all the cases. The evaporation pressure in design conditions was set equal to the optimum values, based on the design thermodynamic results described in paragraph 4.1. The input variables for the three analyzed layouts (see Table 1) were varied in order to simulate the ORC performance under variable DH heat demand.

Figure 10 shows the ORC net power output as a function of different considered input variables, namely the IHTF HE inlet/outlet gas temperature and inlet mass flow, for the different layout arrangements. The input variables ranged between the 110% design load condition and the minimum possible operating value. In detail, Figure 10a shows the performance behavior of Case A layout as a function of the temperature of the exhaust gas feeding the IHTF HE (T_{G2}, see Figure 6), for the different IHTF design temperature. The figure indicated that sizing the ORC on higher IHTF design temperature improved the power production in design conditions, but affected the performance in off-design and limited the operational range of the ORC. Indeed, in Case A1, the ORC could exploit exhaust gas temperature values down to 310 °C; for the Case A2, down to 260 °C; for the Case A3, down to 240 °C. Figure 10b shows the performance of Case B layout as a function of the gas outlet temperature (T_{G2}, see Figure 6), while, in Figure 10c, ORC power output was plotted versus the gas mass flow rate ($\dot{m}_{G1''}$, see Figure 6). In Case B, the exhaust gas outlet temperature ranged between 190 °C and 320 °C. In Case C, the ORC could operate with gas mass flow ranging between 12 and 36 kg/s.

Actually, an ORC could be regulated from full-load down to minimum 30% continuously with fast response, while it was able to increase its power output, up to 110% of its rated power, for a limited amount of hour. Thus, in this analysis, it was assumed that the ORC could work during the year even in the moments when the heat demand was lower than 3 MW, when the IHTF HE was fed with a thermal power higher than the design one until the ORC load did not exceed the 110%.

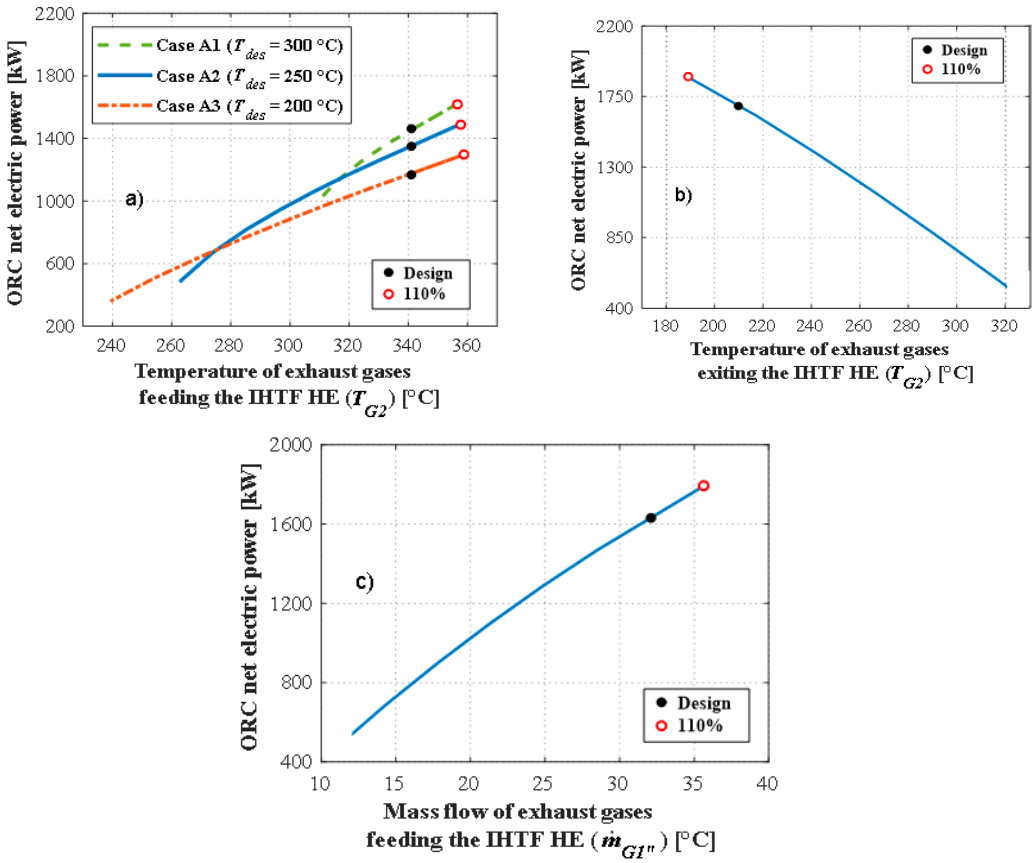

Figure 10. ORC net electric power at part-load conditions: (**a**) effect of gas temperature at IHTF HE inlet, for layout A and different T_{des} values; (**b**) effect of gas temperature at IHTF HE outlet, for layout B; (**c**) effect of gas mass flow.

4.3. Energy Evaluation

According to the DH yearly heat demand profile of Figure 2 and to the ORC performance trends of Figure 10, main comparative energy results were quantified and summarized in Table 7, showing the yearly fuel consumption and ICE generated energy, the ORC design and peak power output, the ORC average power during operating hours, the ORC yearly generated electrical energy, the ORC + ICEs yearly generated electrical energy, and additional generated energy, for each analyzed case study. The number of operating hours and generated electric power output for each investigated layout are also shown and compared in Figure 11, in the form of power outputs monotonic profiles. The ORC performance referred to the net ORC electric power output obtained as gross electric power output value minus IHTF and ORC pumps consumptions (corresponding to about the 8% of the ORC gross electric power output), minus air condenser fan consumptions (corresponding to another 8% of the ORC gross electric power output alone).

In the new arrangement, the ICEs worked the whole year at full-load, producing more energy than in the original set-up, in which they often operate at part-load conditions following the heat demand. In particular, in the new arrangement, the ICEs produced 170.89 GWh/years of additional electric energy, consuming 344.59 GWh/years of fuel more than in the original set-up. The exhaust gas was recovered, furthermore, to feed the IHTF HE, and an additional amount of energy was produced by means of the ORC. Therefore, the total electric energy produced by the new arrangement depended on the considered ORC layout performance.

Table 7. Main energy results for the analyzed configurations.

Comparative Results	Original Arrangement		New Arrangements	Difference	
Fuel consumption, *F* (GWh/year)	138.36		482.95	344.59	
ICE generated electric energy (GWh/year)	54.22		225.11	170.89	
Generated thermal energy (GWh/year)	50.05		50.05	0	
ORC Results	**CASE A1**	**CASE A2**	**CASE A3**	**CASE B**	**CASE C**
Design ORC power output (kW)	1465	1360	1183	1996	1627
Maximum ORC power output (kW)	1573	1496	1301	2027	1790
ORC average power during operating hours (kW)	1433	1177	988	1617	1451
ORC generated electric energy (GWh_e/year)	6.34	7.10	5.51	5.06	9.77
ORC + ICEs generated electric energy (GWh_e/year)	231.45	232.21	230.62	230.17	234.88
Additional generated electric energy, ΔE_{EL} [GWh_e/year] (a+b)	177.23	177.99	176.40	175.95	180.66
GPES (%)	17.9	18.2	17.6	17.4	19.1

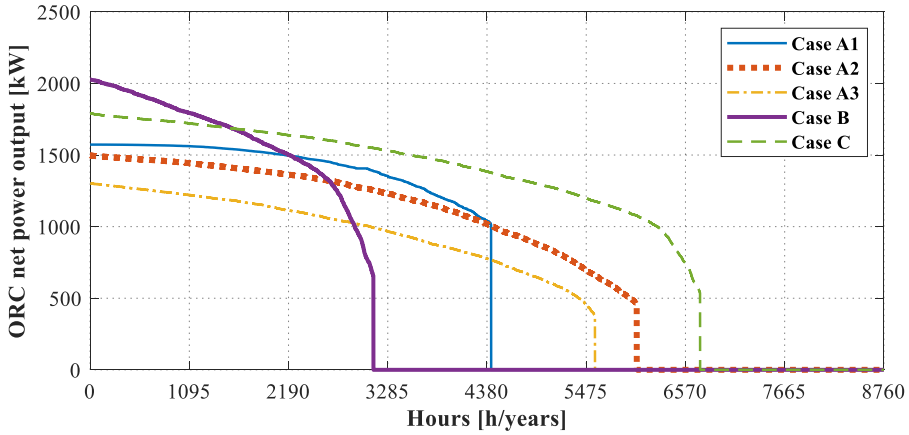

Figure 11. Power output monotonic profiles during the year for each investigated layout.

Case B showed the highest ORC power peak value, but not the highest amount of producible electric energy, due to the limited number of hours in which it operates during the year (about 3126). Thus, in order to evaluate the performance of the ORC on the year basis, it was fundamental to analyze its behavior also at part-load conditions and to take into account its regulation limits. In this case study, the number of operating hours turned out to be fundamental: the layout that allowed to produce the maximum amount of ORC electric energy per year, 9.77 GWh/year, was the Case C, case where the ORC could operate for the greatest number of hours, equal to 7050 h/year. More detailed results concerning the ORC best case (Case C) are reported in Appendix A for completeness. In particular, the monthly profile of heat demand, electric power generated by the old arrangement and the new one, and ORC net electric power output are grouped in Figure A1. Daily profile of heat demand and ORC net electric power output are presented and compared in Figure A2, for two days (February 15th and July 15th), chosen as representative of winter and summer operations of the DHN.

In order to measure the benefits of the ICE-ORC CHP production, a comparison was carried out between two scenarios, in terms of primary energy consumption: in the first scenario, the old CHP system was considered, while, in the second scenario, the new CHP was considered, where an additional electric energy production (ΔE_{EL}) occurred, and heat demand remained the same (see Table 7).

A relative global primary energy saving (*GPES*) could be calculated as follows:

$$GPES = \frac{F_{old} - F_{new}}{F_{old}} \quad (2)$$

where F_{old} is the primary energy consumption in the old scenario, and F_{new} is the primary energy consumption in the second one, respectively, calculated according to Equation (3) and Equation (4).

$$F_{new} = F_{ICEnew} + F_{BOILERnew} \tag{3}$$

$$F_{old} = F_{ICEold} + F_{BOILERold} + \frac{\Delta E_{EL}}{\eta_{EL\ GEN\ MIX} \cdot p} \tag{4}$$

In particular, the primary energy consumption could be split into three contributions: a contribution due to the ICEs operation, F_{ICE}, a contribution due to the boiler's operation, F_{BOILER}, and a third term due to, ΔE_{EL}. This term represented the fuel saved by producing ΔE_{EL} with the new arrangement in place of external electric energy production, and it was calculated considering the European electric generating mix. This latest contribution was estimated as the ratio between the additional generated electric energy from the engines and the ORC, ΔE_{EL}, and the average electric efficiency of the European electric generating mix, $\eta_{EL\ GEN\ MIX}$, and a coefficient, p, which took into account the grid losses depending on the feed-in voltage connection to the grid; in particular, p was intended to promote the feed-in of electricity at lower voltage.

In this analysis, $\eta_{EL\ GEN\ MIX}$ was assumed equal to 40%, which corresponded to the EU28 average electric efficiency of the electric generating mix in 2017 [25]. p was assumed equal to 0.985, which corresponded to the correction factor related to the avoided grid losses, for a CHP system connected to the grid at a voltage equal to 150 kV, as provided by the Directive on primary energy-saving calculation [26].

Results concerning the *GPES* are also reported in Table 7. The *GPES* analysis highlighted that the ICE-ORC arrangement introduced a positive primary energy saving. The *GPES*, however, differed for the different analyzed configuration; in particular, the highest value of the *GPES* was obtained for the Case C (19.1%), while the lowest value was obtained for the Case B (17.4%), for the aforementioned reasons. The inclusion of the ORC entailed positive values of *GPES* mainly because it allowed producing additional electric energy with remarkably high-efficiency values close to 52%, higher than the considered average European electric generating mix efficiency and in line with the current technology of mid-size combined cycles.

4.4. Techno-Economic Feasibility of Analyzed ICE-ORC Layouts

The ICE-ORC solution was compared to the original arrangement in terms of economic performance, by means of the differential net present value index. The differential net present value is defined in Equation (5), where ΔC_i is the differential cost, ΔR_i is the differential revenue at the i-th year, M_a is a factor assumed equal to 0.9 [27] that accounts for the ORC yearly maintenance costs, q is the discount rate assumed equal to 6%, and I_{ORC} is the investment on the ORC system. The differential cost was evaluated as the product between the natural gas price and the differential primary energy consumption (Equation (6)). Different gas price values were considered in this analysis: a medium value assumed equal to 33 EUR/MWh, a high value equal to 44 EUR/MWh, and a low value equal to 22 EUR/MWh. These values corresponded, respectively, to the average, the highest, and the lowest natural gas price encountered in the European countries at the beginning of 2019 [28]). The differential revenue was estimated according to Equation (7) as the product between the electric energy sell price and the differential generated energy. The investment cost of ORC was quantified according to the trend line in Figure 12, where specific investment cost was plotted as a function of the ORC size, based on product data of an ORC market leader manufacturer [23].

Equation (8) could be manipulated in order to evaluate the electric energy price that guarantees the return on investment in a given time period, i.e., the payback period (*PB*), using Equation (5).

$$\Delta NPV = \sum_{i=1}^{n} \frac{\Delta R_i \cdot M_a - \Delta C_i}{(1+q)^i} - I_{ORC} \tag{5}$$

$$\Delta C_i = \Delta F \cdot C_{FUEL} \tag{6}$$

$$\Delta R_i = \Delta E_{EL} \cdot C_{EL} \tag{7}$$

$$C_{EL} = \left(\frac{I_{ORC}}{\sum_{i=1}^{PB} \frac{1}{(1+q)^i} \cdot PB} + \Delta C_i \right) \cdot \frac{1}{\Delta E_{EL} \cdot M_a} \tag{8}$$

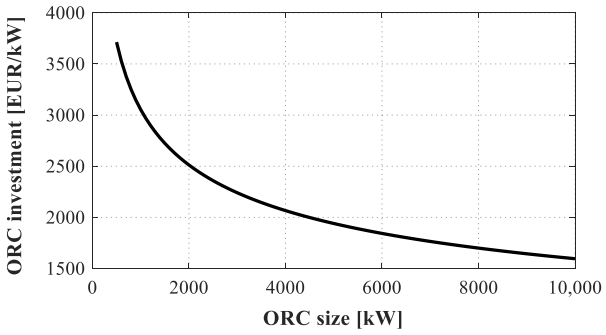

Figure 12. ORC specific investment cost as a function of plant size [23].

Figure 13 displays the results of the economic assessment in terms of electric energy sell price to return on investment in a given payback period. In particular, Figure 13a shows a comparison between the different ICE + ORC layouts, by considering the same natural gas price (the medium value), while Figure 13b shows the influence of the natural gas price. As expected, the payback period decreased when the electric energy price increased; indeed, higher electric energy prices led to higher revenues and, thus, to lower payback periods.

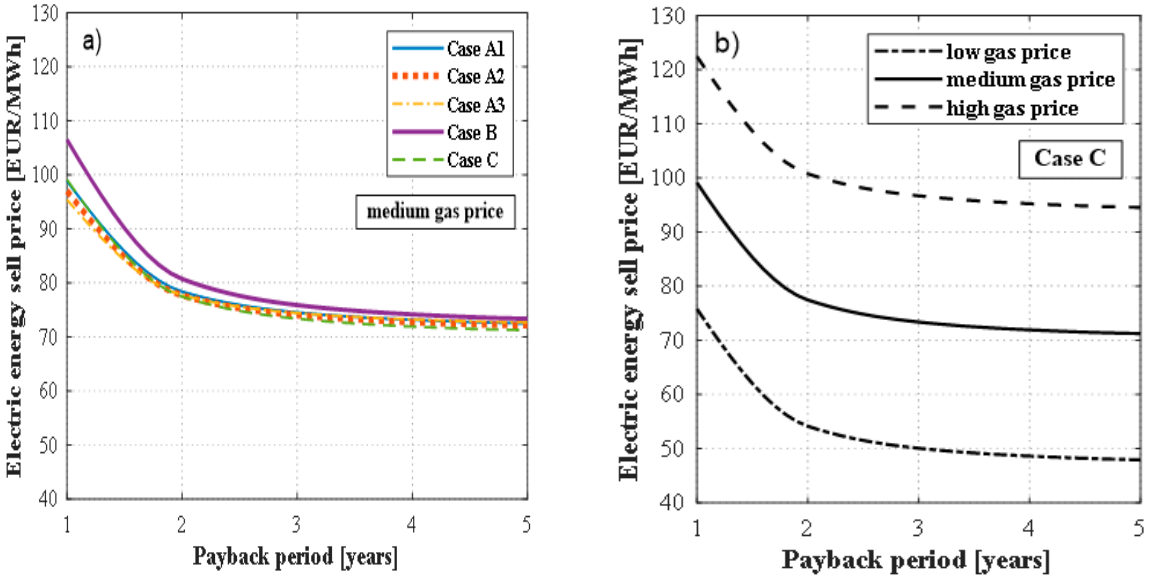

Figure 13. Electric energy sell price to return on the investment in a given payback period: (**a**) Comparison between the different ICE + ORC configurations; (**b**) Influence of the natural gas price value.

The trends were very similar for the different layouts, only Case B deviated slightly from the others. From the economic point of view, the Case B was the worst one because it presented the highest investment (due to the highest size) and the lowest yearly earning (due to the lowest yearly energy production). In general, the ORC solution proved to be a good investment since it allowed returning on the investment in barely 5 years, by selling the electric energy at a price of about 70 EUR/MWh,

considering a medium natural gas price (33 EUR/MWh). When the higher natural gas price was considered, instead, the electric energy sell price could be lower in order to return on the investment in the same payback period; when lower natural gas price was considered, on the contrary, the electric energy sell price must increase. Especially for the Case C, in order to return on the investment in 5 years, the electric energy should be sold at a price of 95 EUR/MWh, considering the high gas price, or at a price of even 50 EUR/MWh, considering the low gas price.

5. Conclusions

This paper investigated the possibility of adding supplementary electric energy production to a CHP system at a service of a DHN, by converting the prime movers' exhaust heat with an ORC. The inclusion of the ORC allowed operating the prime movers at full-load (thus at their maximum efficiency), regardless of the heat demand, without dissipating not required high enthalpy-heat. Indeed, discharged heat was recovered by the ORC to produce additional electric power at high efficiency. In this work, a specific case study of an existing CHP system was analyzed; however, the same presented approach and similar considerations could be applied to any CHP feeding a DHN as a thermal user.

In the original arrangement, three internal combustion engines covered the heat demand together with the back-up boilers. ICEs load regulation strategy was determined in order to fulfill the DH demand while minimizing the heat dissipation to the ambient. The CHP in its original arrangement was compared to a new arrangement, including an ORC. In the new set-up, the ICEs worked at full-load for the whole year. The ORC was conceived to exploit the residual heat of the internal combustion engine exhaust gases, which has not been used by the district heating in part-load conditions. Three distinct layouts were investigated in this work: i) the ORC placed downstream the heat exchanger feeding the DH network; ii) the ORC supposed to be upstream the DH heat exchanger; iii) a parallel arrangement.

A sensitivity analysis of organic fluid and key cycle parameters was performed in order to identify, for each proposed arrangement, the optimum design of the ORC. Results showed that, for each analyzed configuration, Cyclopentane achieved the best performance compared to other hydrocarbons. The value of the optimal evaporation pressure depended on the considered configuration. As expected, the highest ORC performance was achieved for the highest value of the intermediate heat-transfer fluid circuit design temperature. Maximum power output (2027 kW) was achieved for the second layout solution, with an evaporation pressure of 40 bar and IHTF design temperature equal to 300 °C. In this case, the IHTF heat exchanger was fed with the exhaust gas at its highest temperature and mass flow, if compared with the other case studies. Based on sensitivity analysis results, the CHP-ORC hybrid plants were simulated by means of the commercial software *Thermoflex*™ in design and in off-design conditions to account for ORC and DH part-load operation during the year.

The original optimal operation of the CHP plant was compared with the modified one in order to estimate, for each proposed integrated ICEs-ORC arrangement, the amount of additional generated electric power and the corresponding increase in primary energy consumption. The additional electrical energy produced during the year, thanks to the ORC, its operating hours, and total investment costs were quantified and compared among analyzed layouts. Results showed that the performance of the ORC, on the year basis, strongly depended on its part-load behavior and on its regulation limits. Indeed, even if the second layout exhibited the highest ORC power peak value, in design conditions, it did not provide the highest amount of producible electric energy on the year basis because of the limited number of hours in which it operated during the year. The layout that allowed to produce the maximum amount of ORC electric energy per year, 9.77 GWh/year, was the third one, i.e., the parallel arrangement. In the third set-up, the ORC peak power was lower than in the second (1790 kW), but it could operate for the greatest number of hours, namely 7050 h/year. Thus, the actual number of operating hours during the year, determined by the ORC regulation limits, turned out to be fundamental in the plant arrangement decision. An energetic index accounting for the global primary energy saving was introduced, in order to evaluate the convenience in producing the additional electric power with the modified CHP plant rather than with the original plant with the help of the electric

generating mix. The energetic analysis demonstrated that all the proposed solutions granted to reduce the global primary energy consumption by about 18%. The best ICE + ORC solution, in particular, introduced a positive global primary energy saving equal to 19.1%. The inclusion of the ORC entailed significant savings in primary energy consumption because it allowed producing electric energy with an efficiency close to 52%, higher than the electric generating mix efficiency.

Finally, the economic feasibility of each CHP-ORC hybrid system layout was evaluated. The differential cost between the original and the new arrangement was related to the additional primary energy consumption. The differential revenue, instead, was proportional to the additional generated energy. The economic analysis showed that the second layout was the worst solution since it presented the highest investment (due to the highest size) and the lowest yearly earning (due to the lowest yearly energy production). Nevertheless, all the proposed ORC solutions proved to be a good investment since they allowed to return on the investment in barely 5 years, by selling the electric energy at a price equal to 70 EUR/MWh, considering a medium natural gas price equal to 33 EUR/MWh. When the higher natural gas price was considered, instead, the electric energy sell price could be lower in order to return on the investment in the same payback period; when lower natural gas price was considered, on the contrary, the electric energy sell price must increase. Especially for the best ICE+ORC case, in order to return on the investment in 5 years, the electric energy could be sold at a price of 95 EUR/MWh, considering the high gas price, or at a price of even 50 EUR/MWh, considering the low gas price.

In conclusion, results of this work allowed to state that the ORC technology effectively represents an interesting solution to make the plant regulation more flexible, with the purpose of optimizing economic revenue and energetic performance of the CHP plant, while not dissipating high-enthalpy valuable heat to the ambient. Given the promising results of this work, future studies will be dedicated to investigating the dynamic behavior of the DHN, by considering also thermal storage, in order to evaluate the possibility of managing the DHN in a more active and profitable way.

Author Contributions: Conceptualization, L.B. and F.M.; Data curation, N.T.; Funding acquisition, F.M.; Methodology, L.B. and F.M.; Project administration, A.D.P.; Software, N.T.; Supervision, L.B., A.D.P., and F.M.; Validation, A.D.P.; Writing—original draft, N.T.; Writing—review and editing, A.D.P. All authors have read and agreed to the published version of the manuscript.

Funding: This research received no external funding.

Conflicts of Interest: The authors declare no conflict of interest.

Nomenclature

Acronyms

CHP	Combined heat and power
DH	District heating
DHN	District heating Network
GR	Group
GPES	Global primary energy saving
HE	Heat exchanger
ICE	Internal combustion engine
IHTF	Intermediate heat transfer fluid
ORC	Organic Rankine cycle
WHR	Waste heat recovery

Symbols

Δ	Differential
C	Cost (EUR)
E	Energy (GWh)
f	Function of (-)
I	Investment costs (EUR)
M_a	Maintenance cost factor (-)
$\dot{m}$	Mass flow (kg/s)

n	Plant operating life (years)
η	Efficiency (%)
PB	Payback period (years)
q	Discount rate (%)
$\dot{Q}$	Thermal power (W)
R	Revenue (EUR)
T	Temperature (°C)
Subscripts	
des	Design
diss	Dissipated
el	Electric
exhaust	Exhaust
fuel	Fuel
max	Maximum
new	New
old	Old
th	Thermal

Appendix A

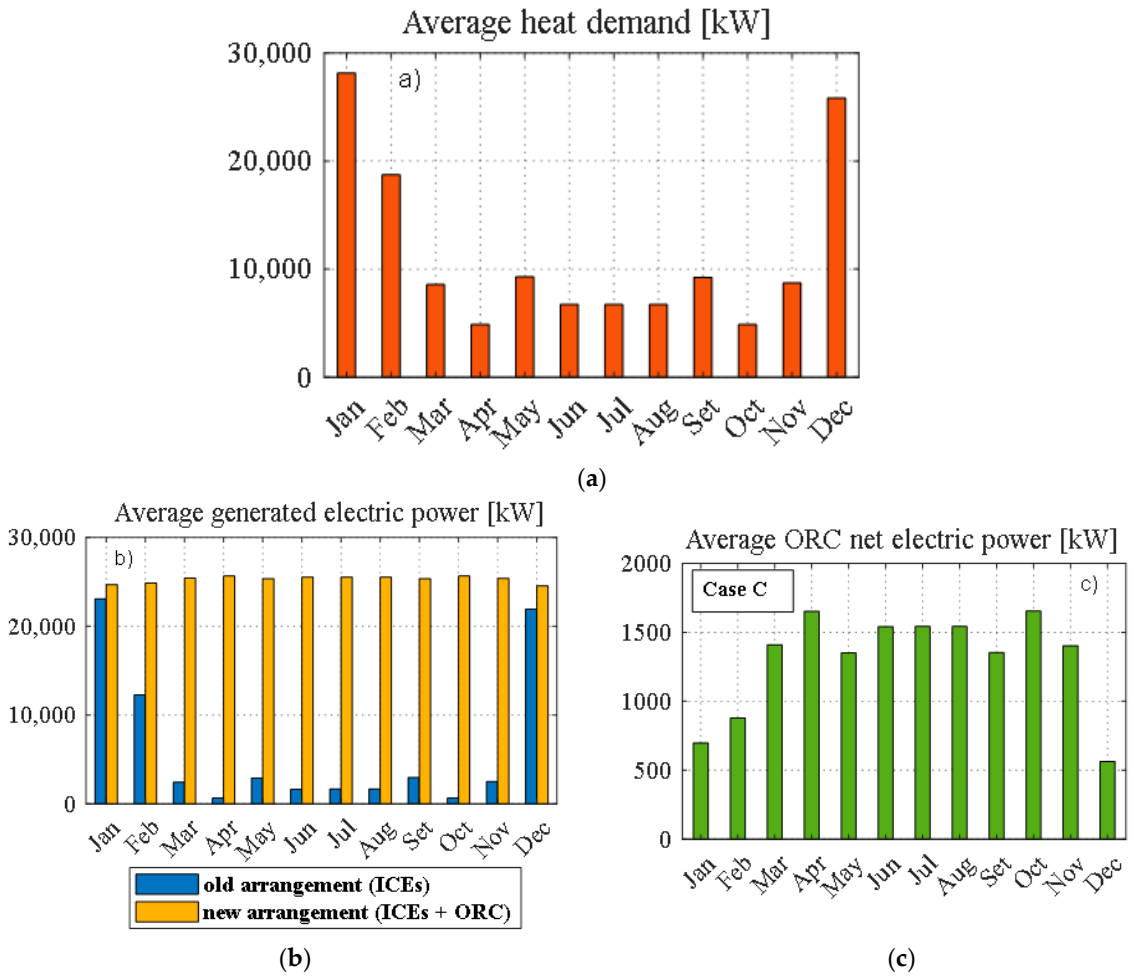

Figure A1. Monthly profile of: (**a**) Thermal power demand; (**b**) Electric power generated by the old arrangement and the new one; (**c**) ORC net electric power output.

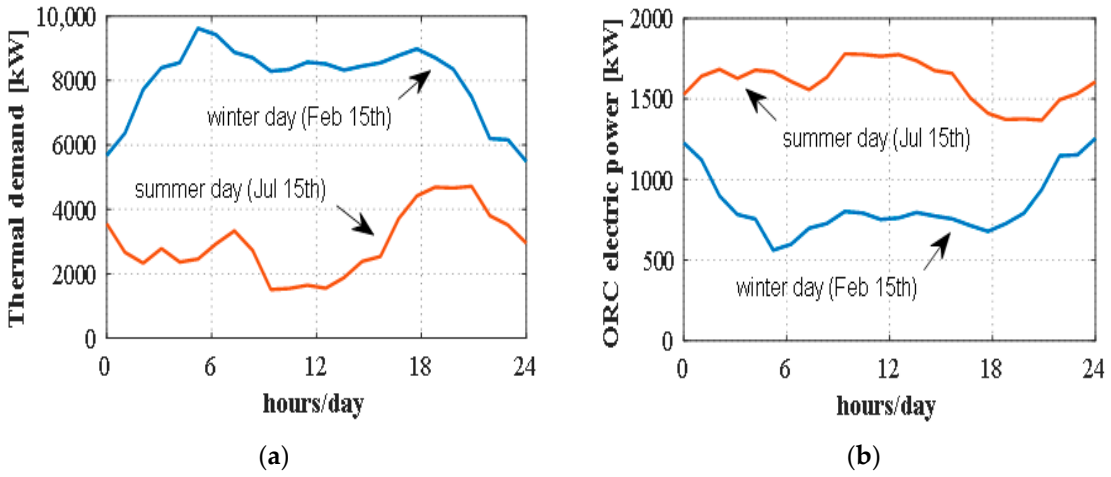

Figure A2. Daily profile of Thermal demand and ORC net electric power output for two representative days: (**a**) 15th of February; (**b**) 15th of July.

References

1. European Commission. Energy Efficiency Directive. 2019. Available online: https://ec.europa.eu/energy/en/topics/energy-efficiency/targets-directive-and-rules/energy-efficiency-directive (accessed on 1 December 2019).
2. European Commission. EU 2020 Target for Energy Efficiency. 2019. Available online: https://ec.europa.eu/energy/en/topics/energy-efficiency/targets-directive-and-rules/eu-targets-energy-efficiency (accessed on 1 December 2019).
3. Macchi, E.; Astolfi, M. *Organic Rankine Cycle (ORC) Power Systems—Technologies and Applications*; Woodhead Publishing: Duxford, UK, 2017.
4. Quoilin, S.; Van Den Broek, M.; Declaye, S.; Dewalle, P.; Lemort, V. Techno-economic survey of Organic Rankine Cycle (ORC) systems. *Renew. Sustain. Energy Rev.* **2013**, *22*, 168–186. [CrossRef]
5. Yang, K.; Zhang, H.; Song, S.; Yang, F.; Liu, H.; Zhao, G.; Zhang, J.; Yao, B. Effects of Degree of Superheat on the Running Performance of an Organic Rankine Cycle (ORC) Waste Heat Recovery System for Diesel Engines under Various Operating Conditions. *Energies* **2014**, *7*, 2123–2145. [CrossRef]
6. Han, Z.; Li, P.; Han, X.; Mei, Z.; Wang, Z. Thermo-Economic Performance Analysis of a Regenerative Superheating Organic Rankine Cycle for Waste Heat Recovery. *Energies* **2017**, *10*, 1593. [CrossRef]
7. Valencia, G.; Fontalvo, A.; Cárdenas, Y.; Duarte, J.; Isaza, C. Energy and Exergy Analysis of Different Exhaust Waste Heat Recovery Systems for Natural Gas Engine Based on ORC. *Energies* **2019**, *12*, 2378. [CrossRef]
8. Wang, X.; Tian, H.; Shu, G. Part-Load Performance Prediction and Operation Strategy Design of Organic Rankine Cycles with a Medium Cycle Used for Recovering Waste Heat from Gaseous Fuel Engines. *Energies* **2016**, *9*, 527. [CrossRef]
9. Song, S.; Zhang, H.; Zhao, R.; Meng, F.; Liu, H.; Wang, J.; Yao, B. Simulation and Performance Analysis of Organic Rankine Systems for Stationary Compressed Natural Gas Engine. *Energies* **2017**, *10*, 544. [CrossRef]
10. Yi, J.Y.; Kim, K.M.; Lee, J.; Oh, M.S. Exergy Analysis for Utilizing Latent Energy of Thermal Energy Storage System in District Heating. *Energies* **2019**, *12*, 1391. [CrossRef]
11. Arabkoohsara, A.; Namib, H. Thermodynamic and economic analyses of a hybrid waste-driven CHP–ORC plant with exhaust heat recovery. *Energy Convers. Manag.* **2019**, *187*, 512–522. [CrossRef]
12. Marty, F.; Serra, S.; Sochard, S.; Reneaume, J.M. Simultaneous optimization of the district heating network topology and the Organic Rankine Cycle sizing of a geothermal plant. *Energy* **2018**, *159*, 1060–1074. [CrossRef]
13. Ramireza, M.; Epeldea, M.; Gomez de Artechea, M.A.; Hammerschmidc, P.A.; Baresid, M.; Monti, N. Performance evaluation of an ORC unit integrated to a waste heat recovery system in a steel mill. *Energy Procedia* **2017**, *29*, 535–542. [CrossRef]
14. Grljušić, M.; Medica, V.; Radica, G. Calculation of Efficiencies of a Ship Power Plant Operating with Waste Heat Recovery through Combined Heat and Power Production. *Energies* **2015**, *8*, 4273–4299. [CrossRef]
15. *Thermoflex 27.0*; Thermoflow Inc.: Subdury, MA, USA, 2019.

16. Ancona, M.A.; Melino, F.; Peretto, A. An Optimization Procedure for District Heating Networks. *Energy Procedia* **2014**, *61*, 278–281. [CrossRef]
17. Doty, S.; Turner, C.W. *Energy Management Handbook*, 6th ed.; Taylor and Francis: Lilburn, GA, USA, 2006.
18. Ancona, M.A.; Baldi, F.; Bianchi, M.; Branchini, L.; Melino, F.; Peretto, A.; Rosati, J. Efficiency improvement on a cruise ship: Load allocation optimization. *Energy Convers. Manag.* **2018**, *164*, 42–58. [CrossRef]
19. Shi, L.; Shu, G.; Tian, H.; Deng, S. A review of modified Organic Rankine cycles (ORCs) for internal combustion engine waste heat recovery (ICE-WHR). *Renew. Sustain. Energy Rev.* **2018**, *92*, 95–110. [CrossRef]
20. Zhang, T.; Zhu, T.; An, W.; Song, X.; Liu, L.; Liu, H. Unsteady analysis of a bottoming Organic Rankine Cycle for exhaust heat recovery from an Internal Combustion Engine using Monte Carlo simulation. *Energy Convers. Manag.* **2016**, *124*, 357–368. [CrossRef]
21. Lemmon, E.W.; Bell, I.H.; Huber, M.L.; McLinden, M.O. *NIST Standard Reference Database 23: Reference Fluid Thermodynamic and Transport Properties-REFPROP, Version 10.0*; National Institute of Standards and Technology: Gaithersburg, MD, USA, 2010; Volume 22.
22. Therminol 62 Brochure. Available online: https://www.therminol.com/sites/therminol/files/documents/TF-8692_Therminol_62.pdf (accessed on 1 December 2019).
23. Bianchi, M.; Branchini, L.; De Pascale, A.; Melino, F.; Peretto, A.; Archetti, D.; Campana, F.; Ferrari, T.; Rossetti, N. Feasibility of ORC application in natural gas compressor stations. *Energy* **2019**, *173*, 1–15. [CrossRef]
24. Bianchi, M.; Branchini, L.; De Pascale, A.; Melino, F.; Orlandini, V.; Peretto, A.; Archetti, D.; Campana, F.; Ferrari, T.; Rossetti, N. Energy recovery in natural gas compressor stations taking advantage of organic Rankine cycle: Preliminary design analysis. In Proceedings of the ASME Turbo Expo 2017, Charlotte, NC, USA, 26–30 June 2017.
25. Electric Generation Mix Efficiency Data. *Fattori di Emissioni Atmosferica di Gas a Effetto Serra Nel Settore Elettrico Nazionale e Nei Principali Paesi Europei*; ISPRA: Rome, Italy, 2019; p. 69.
26. Correction Factor Related to the Losses Avoided Along the Grid, for a Chp System. Data Available from Italian Ministerial Decree Related to Combined Heat and Power Primary Energy Saving Calculation: Allegato VII del DM 4 Agosto 2011 GSE—Cogenerazione ad Alto Rendimento. Available online: https://www.gazzettaufficiale.it/eli/id/2011/09/19/11A12046/sg (accessed on 1 December 2019).
27. Bianchi, M.; Branchini, L.; De Pascale, A.; Melino, F.; Orlandini, V.; Peretto, A.; Archetti, D.; Campana, F.; Ferrari, T.; Rossetti, N. Techno-Economic Analysis of ORC in Gas Compression Stations Taking into Account Actual Operating Conditions. *Energy Procedia* **2017**, *129*, 543–550. [CrossRef]
28. Eurostat. Natural Gas Price Statistics. 2019. Available online: https://ec.europa.eu/eurostat/statistics-explained/index.php/Natural_gas_price_statistics#Natural_gas_prices_for_non-household_consumers (accessed on 1 December 2019).